Electrochemical Impedance of Ion–Exchange Membranes in Ternary Solutions with Two Counterions

ARTICLE *in* THE JOURNAL OF PHYSICAL CHEMISTRY C · FEBRUARY 2014

Impact Factor: 4.77 · DOI: 10.1021/jp4108238

1 AUTHOR:

A.A. Moya
Universidad de Jaén
37 PUBLICATIONS **315** CITATIONS

THE JOURNAL OF PHYSICAL CHEMISTRY C

Article

pubs.acs.org/JPCC

Electrochemical Impedance of Ion-Exchange Membranes in Ternary Solutions with Two Counterions

A. A. Moya*

Departamento de Física, Universidad de Jaén, Edificio A-3, Campus Universitario de Las Lagunillas - 23071 Jaén, Spain

ABSTRACT: This paper aims to study the electrochemical impedance of a system consisting of an ion-exchange membrane and two diffusion boundary layers on both sides of the membrane bathed in ternary electrolyte solutions with two counterions. An approximate analytical expression has been arranged for the impedance of an ideal ion-exchange membrane system for counterions with identical charge number on the basis of the Nernst−Planck−Donnan equations under electroneutrality. The electrochemical impedance for different values of the direct electric current of ion-exchange membrane systems with univalent ions has been numerically obtained from the Nernst−Planck and Poisson equations. The results have been compared with the approximate analytical expressions in different arrangements of practical interest, including conventional electrodialysis, bi-ionic conditions, and reverse electrodialysis. Our results provide new insights into the role played by the generalized expressions of the transport numbers, electrolyte diffusion coefficients, limiting electric currents, and membrane resistance in the interpretation of electrochemical impedances of ion-exchange membranes in ternary electrolyte solutions with two counterions. Moreover, new physical insights emerge from the analysis of the conductive contribution to the total impedance of the system.

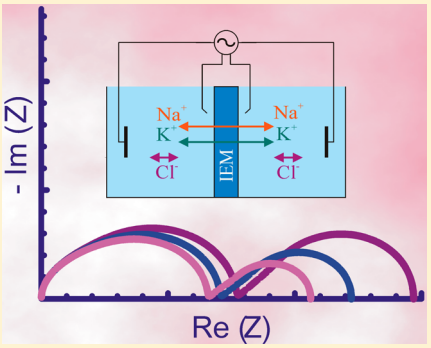

1. INTRODUCTION

Characterization of electrodiffusive ionic transport processes by means of electrochemical impedance spectroscopy techniques is currently a classical issue in physical chemistry. The available numerical simulation programs, precise instrumentation, and interesting technological applications have provided new insights in the field of impedance spectroscopy of ion-exchange membrane systems. Such membranes find a wide range of application in the fields of ion-selective electrodes used as chemical sensors and brackish water or seawater desalination.[1] Recently, there is also an increasing interest in applications for renewable energy sources such as reverse electrodialysis.[2] Moreover, the ion-exchange membranes are used as separators in low-temperature fuel cells and rechargeable batteries, especially in redox flux batteries.[3] An ion-exchange membrane system is constituted by a layer of material with inner electric charge that separates two solution phases. Conventional membranes present fixed or mobile ionic sites, and they are partially permeable or fully impermeable to at least one dissolved ionic component. An ion-exchange membrane is ideal when the fluxes of the co-ions through it are zero.

Since the work of Sistat et al.,[4] a number of papers dealing with the electrochemical impedance of systems constituted by an ion-exchange membrane and two diffusion boundary layers (DBLs) adjacent to the membrane have appeared in the literature. These works include studies on the effect of the displacement electric current,[5] the diffusion coefficients dependent on the ionic concentrations,[6] and the highest values of the direct component of the electric current[7,8] on the impedance of ideal ion-exchange membrane systems by using the Nernst−Planck−Donnan equations under electroneutrality. Moreover, the influence of the capacitance of the diffuse double layers,[9] degree of inhomogeneity of the membrane fixed-charge,[10,11] direct component of the electric current,[12] degree of asymmetry of the bathing concentrations,[13] smallest values of the fixed-charge concentration,[14] and rectangular structure of fluidic nano-channels[15] on the impedance of nonideal ion-exchange membranes have been studied in depth on the basis of the Nernst−Planck and Poisson equations. However, these previous studies deal with only the ionic transport processes of a single binary electrolyte.

Multi-ionic transport through ion-exchange membranes is also of interest, particularly in studies on bi-ionic electric potential of membranes,[16−18] water dissociation in anion-exchange membranes,[19,20] or ionic transport through bipolar membranes.[21,22] Recently, the dynamic of the electric potential in both multi-ionic liquid junctions[23,24] and infinitesimal membranes[25] and the impact of adding salts on the steady-state and transient electrical properties of electrolytic cells[26] and Li-ion rechargeable batteries[27] have also been analyzed. Moreover, a detailed study on the electrochemical impedance of ion-selective electrodes under membrane control, i.e., by ignoring the DBLs adjacent to the membrane, has been presented for multi-ion systems.[28,29]

Although the study of the steady-state multi-ionic electric potential in ion-exchange membrane systems under equilibrium conditions is a classical issue in the literature,[30−35] to our knowledge, theoretical studies on the electrochemical impedance of such systems with at least three dissolved ions have not yet

Received: November 3, 2013
Revised: January 12, 2014
Published: January 15, 2014

dx.doi.org/10.1021/jp4108238 | J. Phys. Chem. C 2014, 118, 2539−2553

been reported. Multi-ionic transport process through ion-exchange membranes is conditioned by the ionic partitioning,[36] but it seems desirable to know the conditions in which the impedance plots can be interpreted by using single electric elements in a way similar to that in binary electrolyte solutions. It is the main purpose of this paper to contribute to this area by performing a novel theoretical study of the characteristics of the electrochemical impedance of ion-exchange membranes immersed in ternary electrolyte solutions with two counterions.

The particular system under study is constituted by a membrane with negative fixed charge and two DBLs on both sides of the membrane, being considered the ionic transport of a mixture of two binary electrolytes with common anion. An approximate analytical expression is arranged for the electrochemical impedance of an ideal ion-exchange membrane system where the counterions present identical charge number on the basis of the Nernst−Planck flux equations, Donnan equilibrium relations at the interfaces, electroneutrality condition, and the hypothesis of constant relative ionic composition of all the species into the DBLs. The electrochemical impedance of an ion-exchange membrane system is also numerically obtained from the Nernst−Planck and Poisson equations including the diffuse double layers at the interfaces by using the network simulation method,[37−39] which is mainly based on a finite difference scheme; it is of a nature similar to those successfully used in mixed conductors[40−42] and batteries.[43,44] The numerical results obtained for the impedance are then compared with the approximate analytical expressions. The steady-state voltage−current characteristics and the electrochemical impedance for different values of the direct electric current of ion-exchange membrane systems are investigated in different situations of practical interest with univalent ions. First, we consider a membrane placed between two solutions with the same chemical composition because these systems find application in the field of conventional electrodialysis. Second, we choose an ion-exchange membrane under bi-ionic conditions because of its interest in the field of electrochemical sensors. Finally, a membrane placed between two solutions with different salt concentrations is considered because this is the appropriate arrangement to obtain a salinity gradient in the field of energy production through reverse electrodialysis.

The obtained numerical results are in good agreement with the approximate analytical solutions, and they show that it is possible to employ the single electric elements used in ion-exchange membranes with binary electrolytes to interpret the electrochemical impedance plots obtained with membranes in ternary solutions, which consist of a high-frequency arc associated with the migration processes and the electric displacement current and a low-frequency arc associated with the electrolyte diffusion process. Our results provide new insights in relation to the use of the generalized expressions of the transport numbers, electrolyte diffusion coefficients, limiting electric currents, and resistance of the membrane in the interpretation of electrochemical impedances of ion-exchange membranes in ternary electrolyte solutions with two counterions. Moreover, new physical insights emerge from the analysis of the conductive contribution to the total impedance of the system, which appears to be significant at values of the dc current close to the limiting current.

2. THEORETICAL BASIS

2.1. Ionic Transport in Ion-Exchange Membrane Systems. Let us consider an ion-exchange membrane that extends from $x = 0$ to $x = d$ and two DBLs adjacent to the membrane lying from $x = -\delta_L$ to $x = 0$ and from $x = d$ to $x = d + \delta_R$. The membrane is bathed by two bulk solutions constituted by a mixture of two binary electrolytes with a common anion, and it will be assumed to have a negative fixed-charge. Ionic transport process is supposed to be one-dimensional and perpendicular to the membranelsolution interface, with x the direction of transport. In accord with previous works on ionic transport through ion-exchange membranes,[45−49] the dimensionless equations (see Appendix A) determining the behavior of the system at time t are the laws of mass conservation or continuity equations

$$\frac{\partial J_i(x,\,t)}{\partial x} = -\frac{\partial c_i(x,\,t)}{\partial t}, \qquad i = 1,\,2,\,3 \tag{1}$$

the Nernst−Planck flux equations written for dilute solutions

$$J_i(x,\,t) = -D_{ip}\left[\frac{\partial c_i(x,\,t)}{\partial x} + z_i c_i(x,\,t)\frac{\partial \phi(x,\,t)}{\partial x}\right] \tag{2}$$

and the Poisson equation

$$\frac{\partial \mathbf{D}(x,\,t)}{\partial x} = \left[\sum_{i=1}^{3} z_i c_i(x,\,t)\right] - \theta(x) \tag{3}$$

where

$$\mathbf{D}(x,\,t) = \varepsilon E(x,\,t) = -\varepsilon\frac{\partial \phi(x,\,t)}{\partial x} \tag{4}$$

Here $J_i(x,t)$, D_{ip}, $c_i(x,t)$, and z_i denote the ionic flux, the diffusion coefficient, the molar concentration, and the charge number of ion i, respectively. We consider the ions $i = 1$ and $i = 2$ to be the cations and $i = 3$ to be the anion. In this work, the ion diffusion coefficients are different in the DBLs and in the ion-exchange membrane, and D_{iS} and D_{iM} stand for the diffusion coefficients of ion i in the solution (S) and membrane (M) phases, respectively. The electric potential is represented by $\phi(x,t)$, electric permittivity by ε, electric displacement by $\mathbf{D}(x,t)$, and electric field by $E(x,t)$. The constants F, R, and T have their usual meanings: Faraday constant, ideal gas constant, and absolute temperature, respectively. $\theta(x)$ is the fixed-charge concentration, which is presumed known and expressed in a general way as a function of position, x. In this case, it is given by

$$\theta(x) = \begin{cases} 0, & -\delta_L \le x < 0 \\ -X, & 0 \le x \le d \\ 0, & d < x \le d + \delta_R \end{cases} \tag{5}$$

where the membrane fixed-charge concentration, X, is assumed to be homogeneously distributed inside the membrane.

On the other hand, the faradaic electric current, I_f, is

$$I_f(x,\,t) = \sum_{i=1}^{3} z_i J_i(x,\,t) \tag{6a}$$

and the displacement electric current, I_d, is given by

$$I_d(x,\,t) = \frac{\partial \mathbf{D}(x,\,t)}{\partial t} = \varepsilon\frac{\partial E(x,\,t)}{\partial t} \tag{6b}$$

Now, the total electric current, I, is the sum of the faradaic and displacement currents

$$I(x,\,t) = I_f(x,\,t) + I_d(x,\,t) \tag{7a}$$

dx.doi.org/10.1021/jp4108238 | J. Phys. Chem. C 2014, 118, 2539−2553

However, from the above equations one obtains

$$\frac{\partial I(x,\,t)}{\partial x} = 0 \tag{7b}$$

i.e., I is not a function of x.[50] Thus, the total electric current can be evaluated at an arbitrary point such as $x = -\delta_L$, and it can be written as

$$I(t) = \sum_{i=1}^{3} z_i J_i(-\delta_L,\,t) + \frac{d\mathbf{D}(-\delta_L,\,t)}{dt} \tag{7c}$$

In order to study the response of the membrane system to an externally applied electric current perturbation, the boundary conditions can be expressed as

$$c_1(-\delta_L,\,t) = c_1^{\,L} = -\frac{z_3}{z_1}\gamma_L c^L \tag{8a}$$

$$c_1(d+\delta_R,\,t) = c_1^{\,R} = -\frac{z_3}{z_1}\gamma_R c^R \tag{8b}$$

$$c_2(-\delta_L,\,t) = c_2^{\,L} = -\frac{z_3}{z_2}(1-\gamma_L)c^L \tag{9a}$$

$$c_2(d+\delta_R,\,t) = c_2^{\,R} = -\frac{z_3}{z_2}(1-\gamma_R)c^R \tag{9b}$$

$$c_3(-\delta_L,\,t) = c_3^{\,L} = c^L \tag{10a}$$

$$c_3(d+\delta_R,\,t) = c_3^{\,R} = c^R \tag{10b}$$

$$\frac{d\mathbf{D}(-\delta_L,\,t)}{dt} = I(t) - \sum_{i=1}^{3} z_i J_i(-\delta_L,\,t) \tag{11a}$$

$$\phi(d+\delta_R,\,t) = 0 \tag{11b}$$

eqs 8−11 specify all the conditions to be imposed on the solution of the Nernst−Planck and Poisson equations. In these equations, c^L and c^R are the total concentrations of the common co-ion into the left and right solutions, while γ_L and γ_R are the ratios of the bathing concentration of the binary electrolyte containing the counterion of charge z_1 to the total anion concentration in the left and right solutions, respectively. In this way, eqs 8−10 indicate that the system is electrically neutral at the outer boundaries of the DBLs. In eq 11a, $I(t)$ is the externally applied electric current, and it is used to calculate the value of the electric displacement at the outer boundary of the left DBL. Equation 11b defines the reference level for the electric potential at the outer boundary of the right DBL.

2.2. Electric Current Perturbation. It is well-known that under small-signal ac conditions, the system variables may be separated into steady-state and time-dependent parts by using the algebra of complex numbers. In particular, the co-ion concentration and the electric potential can be written as

$$c_3(x,\,t) = c_{DC}(x) + c_0(x)e^{j\omega t} \tag{12a}$$

$$\phi(x,\,t) = \phi_{DC}(x) + \phi_0(x)e^{j\omega t} \tag{12b}$$

where $j = (-1)^{1/2}$ is the imaginary unit and ω is the circular or angular frequency, which can be written as a function of the conventional frequency, f

$$\omega = 2\pi f \tag{13}$$

To study the electrochemical impedance, the externally controlled electric current through the system is expressed as

$$I(t) = I_{DC} + I_0 e^{j\omega t} \tag{14a}$$

and the electric potential at the outer boundary of the left DBL, $\phi_M(t) = \phi(-\delta_L t)$, can be written as

$$\phi_M(t) = \phi_{MDC} + \phi_{M0}e^{j\omega t} \tag{14b}$$

The electrochemical impedance, Z, is a complex quantity given by the following equation:[51]

$$Z(j\omega) = \frac{\phi_{M0}}{I_0} \tag{15a}$$

and it can be expressed in the Euler or polar and rectangular forms as follows:

$$Z(j\omega) = |Z|e^{j\phi} = Z_r(\omega) + jZ_i(\omega) \tag{15b}$$

where $|Z|$, φ, Z_r, and Z_i are modulus, phase, and real and imaginary parts of the impedance, respectively.

3. IDEAL ION-EXCHANGE MEMBRANE SYSTEMS

3.1. General Governing Equations. Single analytical expressions for a great number of variables can be easily obtained in an ideal membrane system, i.e., a system with a membrane fully impermeable to the co-ions, by assuming the general following hypothesis:[52,53]

- Electrical neutrality into the two DBLs and the membrane.
- Constant relative ionic composition of all the species in the DBLs.
- Zero co-ion flux through the membrane.
- Constant and linearly varying with position concentrations of the counterions inside the membrane, if they present identical valence.
- Electric potential obeying the Donnan equilibrium relations at the two membrane−solution interfaces.

3.1.1. Diffusion Boundary Layers. We will denote by c the anionic (co-ion) concentration, and we will suppose that the ionic concentrations in a DBL present the relative proportion that is the same as that in the bathing solution:

$$c_1 = -\frac{z_3}{z_1}\gamma_K c \quad c_2 = -\frac{z_3}{z_2}(1-\gamma_K)c \quad c_3 = c \tag{16}$$

If we define the transport number of ion i in the solution K (K = L for the left and K = R for the right solution), t_{iK}, as the ratio of the conductivity of ion i to that of the solution

$$t_{iK} = \frac{z_i^2 c_i D_{iS}}{\sum_{i=1}^{3} z_i^2 c_i D_{iS}} \tag{17a}$$

the following relation is obeyed:

$$t_{1K} + t_{2K} + t_{3K} = 1 \tag{17b}$$

So, from eqs 2−4 and 6a, one obtains that the electric field in the DBL K, E_K, is given by

$$E_K = \frac{D_{3S} - \gamma_K D_{1S} - (1-\gamma_K)D_{2S}}{z_3 D_{3S}} t_{3K}\frac{dc}{cdx} + \frac{t_{3K}}{z_3^2 c D_{3S}} I_f \tag{18}$$

the co-ion flux obeys the continuity equation

dx.doi.org/10.1021/jp4108238 | J. Phys. Chem. C 2014, 118, 2539−2553

$$\frac{\partial J_3}{\partial x} = -\frac{\partial c}{\partial t} \tag{19a}$$

and it can be written as

$$J_3 = -D_{SK}\frac{dc}{dx} + \frac{t_{3K}}{z_3}I_f \tag{19b}$$

where D_{SK} is the electrolyte diffusion coefficient in the DBL K, and it is given by

$$D_{SK} = (z_1 - z_3)\frac{D_{3S}t_{1K}}{z_1} + (z_2 - z_3)\frac{D_{3S}t_{2K}}{z_2} \tag{20}$$

3.1.2. Membrane. Because the concentrations of the counterions inside the membrane, $\overline{c_1}$ and $\overline{c_2}$, are related by means of the electrical neutrality condition

$$z_1\overline{c_1} + z_2\overline{c_2} = X \tag{21}$$

the ionic transport inside the membrane can be described by the following equations:

$$\frac{\partial J_1}{\partial x} = -\frac{\partial \overline{c_1}}{\partial t} \tag{22a}$$

and

$$J_1 = -D_{1M}\frac{\partial \overline{c_1}}{\partial x} + z_1 D_{1M}\overline{c_1}E_m \tag{22b}$$

where E_m is now the electric field inside the membrane and it is related with the faradaic electric current through the system by

$$I_f = -z_1(D_{1M} - D_{2M})\frac{\partial \overline{c_1}}{\partial x} + (z_1^2 D_{1M}\overline{c_1} + z_2 D_{2M}X - z_1 z_2 D_{2M}\overline{c_1})E_m \tag{23}$$

Now we can calculate the ionic concentrations at the inner boundaries of the membrane, $\overline{c_1(0)}$ and $\overline{c_1(d)}$, from the electrical neutrality condition

$$\begin{aligned} z_1\overline{c_{1L}} + z_2\overline{c_{2L}} &= X \\ z_1\overline{c_{1R}} + z_2\overline{c_{2R}} &= X \end{aligned} \tag{24a}$$

and the Donnan equilibrium relations at the interfaces

$$\begin{aligned} \frac{1}{z_1}\ln\frac{\overline{c_{1L}}}{c_1(0)} &= \frac{1}{z_2}\ln\frac{\overline{c_{2L}}}{c_2(0)} \\ \frac{1}{z_1}\ln\frac{\overline{c_{1R}}}{c_1(d)} &= \frac{1}{z_2}\ln\frac{\overline{c_{2R}}}{c_2(d)} \end{aligned} \tag{24b}$$

It is a well-known fact that the properties of the ionic transport processes through membranes strongly depend of the charge number of the ions because of the ionic partition at the interfaces. If both counterions present identical value of the charge number, $z_1 = z_2$, the ionic partitioning is

$$\begin{aligned} \overline{c_{1L}} &= \gamma_L\frac{X}{z_1} \quad \overline{c_{2L}} = (1-\gamma_L)\frac{X}{z_1} \\ \overline{c_{1R}} &= \gamma_R\frac{X}{z_1} \quad \overline{c_{2R}} = (1-\gamma_R)\frac{X}{z_1} \end{aligned} \tag{24c}$$

whatever the remaining conditions may be. In this situation, the ionic concentrations inside the membrane are not a function of time. At this point, it must be noted that the partition coefficients have not been incorporated into the theoretical description for the sake of simplicity. In fact, it has been considered that the specific ionic partition coefficients between the external and the membrane solutions are unity.[36]

3.2. Steady State. Because an ideal membrane system is that in which the co-ion flux is zero, from eq 19b one obtains in the steady state

$$\frac{dc}{dx} = \frac{t_{3K}}{z_3 D_{SK}}I_{DC} \tag{25a}$$

The limiting electric current in a DBL is obtained when the steady-state concentration gradient reaches its maximum value in that DBL. From eq 25a with $c(x = -\delta_L) = c^L$ and $c(x = 0) = 0$ or with $c(x = d) = 0$ and $c(x = d + \delta_R) = c^R$, one obtains that the limiting electric current in the DBL K is:

$$I_K = -\frac{z_3 D_{SK}c^K}{t_{3K}\delta_K} \tag{25b}$$

and eq 25a can be written as

$$\frac{dc}{dx} = -\frac{I_{DC}c^K}{I_K\delta_K} \tag{25c}$$

If one denotes by β_K the ratio of the dc electric current to its limiting value

$$\beta_K = \frac{I_{DC}}{I_K} \tag{26}$$

from eq 25c, one finds that the anionic concentration in the left DBL is

$$c_{DC}(x) = c^L\left(1 - \beta_L\frac{x + \delta_L}{\delta_L}\right) \tag{27}$$

Then, by using eq 18, the electric potential difference in the neutral zone of the left DBL is

$$\phi_{DC}^L = \int_{-\delta_L}^{0} E_L\,dx = \frac{1}{z_3}\ln(1 - \beta_L) \tag{28a}$$

while the Donnan equilibrium potential difference at the left interface is

$$\phi_{DC}^{dL} = \frac{1}{z_1}\ln\frac{\overline{c_{1L}}}{c_1(0)} = \frac{1}{z_2}\ln\frac{\overline{c_{2L}}}{c_2(0)} \tag{28b}$$

Now, the anionic concentration in the right DBL is

$$c_{DC}(x) = c^R\left(1 - \beta_R\frac{x - d - \delta_R}{\delta_R}\right) \tag{29}$$

the electric potential difference in the neutral zone of the right DBL is

$$\phi_{DC}^R = \int_d^{d+\delta_R} E_R\,dx = -\frac{1}{z_3}\ln(1 + \beta_R) \tag{30a}$$

while the Donnan potential difference at the right interface is given by

$$\phi_{DC}^{dR} = \frac{1}{z_1}\ln\frac{c_1(d)}{\overline{c_1(d)}} = \frac{1}{z_2}\ln\frac{c_2(d)}{\overline{c_2(d)}} \tag{30b}$$

On the other hand, the electric potential difference through the membrane is

dx.doi.org/10.1021/jp4108238 | J. Phys. Chem. C 2014, 118, 2539−2553

$$\phi_{DC}^{m} = \int_0^d E_m \, dx \tag{31a}$$

and by supposing that the ionic concentrations vary linearly with position inside the membrane

$$\overline{c_i}(x) = \overline{c_{iL}} + \frac{\overline{c_{iR}} - \overline{c_{iL}}}{d} x \tag{31b}$$

and by using eq 23, one finds

$$\phi_{DC}^{m} = \frac{I_{DC} d + \sum_{i=1}^{2} z_i D_{iM} (\overline{c_{iR}} - \overline{c_{iL}})}{\sum_{i=1}^{2} z_i^2 D_{iM} (\overline{c_{iR}} - \overline{c_{iL}})} \ln \frac{\sum_{i=1}^{2} z_i^2 D_{iM} \overline{c_{iR}}}{\sum_{i=1}^{2} z_i^2 D_{iM} \overline{c_{iL}}} \tag{31c}$$

which coincides with the known expression for the equilibrium membrane potential[34] when $I_{DC} = 0$ and it constitutes an extended expression of the membrane potential to include the polarization concentration. In this way, the steady-state electric potential of the membrane system must be obtained as the sum of the several terms associated with the left DBL, the membrane, and the right DBL

$$\phi_{MDC} = \phi_{DC}^{L} + \phi_{DC}^{dL} + \phi_{DC}^{m} + \phi_{DC}^{R} + \phi_{DC}^{dR} \tag{32a}$$

and it can be expressed as

$$\phi_{MDC} = \left(\frac{1}{z_1} - \frac{1}{z_3}\right) \ln \frac{1 + \beta_R}{1 - \beta_L} + \Delta\phi_1 + \Delta\phi_2 + \phi_{DC}^{m} \tag{32b}$$

where

$$\Delta\phi_1 = \frac{1}{z_1} \ln \frac{\gamma_R c^R}{\gamma_L c^L} = \frac{1}{z_2} \ln \frac{(1 - \gamma_R) c^R}{(1 - \gamma_L) c^L} \tag{32c}$$

and

$$\Delta\phi_2 = \frac{1}{z_1} \ln \frac{\overline{c_{1L}}}{\overline{c_{1R}}} = \frac{1}{z_2} \ln \frac{\overline{c_{2L}}}{\overline{c_{2R}}} \tag{32d}$$

It must be noted that it is preferable to use these two above terms, $\Delta\phi_1$ and $\Delta\phi_2$, in the theoretical description in order to include those situations in which γ_L or γ_R take the values 0 or 1, such as occurs for example with bi-ionic membranes.

One of the more important steady-state values describing the impedance of a system is the dc resistance, which is defined as the derivative of the electric potential with respect the electric current. In the general case, this resistance is difficult to obtain because the ionic concentrations inside the membrane depend on the electric current due to the ionic partitioning. Now, if one considers counterions presenting identical charge number, $z_1 = z_2$, the ionic concentrations inside the membrane are given by the ionic partitioning of eq 24c, they are not a function of the dc electric current, and the dc resistance of the system, R_{DC}, can be expressed as

$$R_{DC} = \frac{d\phi_{MDC}}{dI_{DC}} = \left(\frac{1}{z_1} - \frac{1}{z_3}\right)\left(\frac{1}{I_L(1 - \beta_L)} + \frac{1}{I_R(1 + \beta_R)}\right) + R_M \tag{33a}$$

where the membrane resistance, R_M, is given by

$$R_M = \frac{d}{\sum_{i=1}^{2} z_i^2 D_{iM} (\overline{c_{iR}} - \overline{c_{iL}})} \ln \frac{\sum_{i=1}^{2} z_i^2 D_{iM} \overline{c_{iR}}}{\sum_{i=1}^{2} z_i^2 D_{iM} \overline{c_{iL}}} \tag{33b}$$

Moreover, if we consider a membrane placed between two solutions with identical chemical composition ($\gamma_L = \gamma_R$), the potential difference through the membrane can be obtained from eq 31c, and it is expressed as

$$\phi_{DC}^{m} = -\Delta\phi_2 + R_M I_{DC} \tag{34a}$$

where the resistance of the membrane is

$$R_M = \frac{d}{\sum_{i=1}^{2} z_i^2 D_{iM} \overline{c_{iL}}} \tag{34b}$$

In this way, the steady-state potential of the membrane system can be expressed as

$$\phi_{MDC} = \left(\frac{1}{z_1} - \frac{1}{z_3}\right) \ln \frac{1 + \beta_R}{1 - \beta_L} + \frac{1}{z_1} \ln \frac{c^R}{c^L} + R_M I_{DC} \tag{34c}$$

and the dc resistance of the membrane system is given by eq 33a.

3.3. Alternating Current. *3.3.1. Low Frequency.* In the low-frequency range, the displacement electric current can be considered zero. Then, because the continuity equation for the anion in the DBL K is

$$\frac{\partial c}{\partial t} = -\frac{\partial J_3}{\partial x} = D_{SK} \frac{\partial^2 c}{\partial x^2} \tag{35a}$$

by considering eq 12a, one obtains

$$j\omega c_0 = D_{SK} \frac{d^2 c_0}{dx^2} \tag{35b}$$

and by using the following boundary conditions

$$c_0(x = -\delta_L) = 0 \tag{36a}$$

$$\left(\frac{dc_0}{dx}\right)_{x=0} = -\frac{I_0 c^L}{I_L \delta_L} \tag{36b}$$

the general solution of eq 35b in the left DBL is

$$c_0(x) = -\frac{I_0 c^L}{I_L \alpha_L} \frac{\sinh\left(\alpha_L \frac{x + \delta_L}{\delta_L}\right)}{\cosh \alpha_L} \tag{36c}$$

where

$$\alpha_L = \delta_L \sqrt{\frac{j\omega}{D_{SL}}} = \sqrt{j\omega \Lambda_L} \tag{36d}$$

From eq 28a after several arrangements, is obtained that the ac component of the electric field in the left DBL, E_{L0}, is:

$$E_{L0} = \frac{D_{3S} - \gamma_L D_{1S} - (1 - \gamma_L) D_{2S}}{z_3 D_{3S}} t_{3L} \frac{d}{dx}\left(\frac{c_0}{c_{DC}}\right) + \frac{t_{3L} I_0}{z_3^2 D_{3S} c_{DC}} - \frac{t_{3L} I_{DC}}{z_3^2 D_{3S}} \frac{c_0}{c_{DC}^2} \tag{37a}$$

the electric potential difference in the neutral zone of the left DBL is

$$\phi_0^L = \int_{-\delta_L}^{0} E_{L0} \, dx \tag{37b}$$

dx.doi.org/10.1021/jp4108238 | J. Phys. Chem. C 2014, 118, 2539−2553

while the Donnan potential difference at the left interface can be evaluated only for counterions with identical value of the charge number, $z_1 = z_2$, because in other cases the ionic concentrations inside the membrane are a function of time, and it is given by

$$\phi_0^{dL} = -\frac{1}{z_1}\frac{c_0(x=0)}{c_{DC}(x=0)} = \frac{1}{z_1}\frac{I_0}{I_L(1-\beta_L)}\frac{\tanh\alpha_L}{\alpha_L} \tag{37c}$$

From the integration of eq 37b, one obtains that the impedance of the left DBL is

$$Z_L = \frac{\phi_0^L + \phi_0^{dL}}{I_0} = Z_{dL} + Z_{mL} + Z_{cL} \tag{38a}$$

where the diffusion impedance, Z_{dL}, which comes not only from the diffusion in the DBL but also from the Donnan equilibrium relation, is

$$Z_{dL} = \left(\frac{1}{z_1} - \frac{D_{3S} - \gamma D_{1S} - (1-\gamma)D_{2S}}{z_3 D_{3S}} t_{3L}\right)\frac{1}{I_L(1-\beta_L)}\frac{\tanh\alpha_L}{\alpha_L} \tag{38b}$$

the ohmic impedance, Z_{mL}, is

$$Z_{mL} = -\frac{\delta_L t_{3L}}{z_3^2 D_{3S} c^L}\frac{\ln(1-\beta_L)}{\beta_L} \tag{38c}$$

and the impedance of conduction, Z_{cL}, is

$$Z_{cL} = \frac{t_{3L}\delta_L\beta_L}{z_3^2 D_{3S} c^L}\frac{1}{\alpha_L\cosh\alpha_L}\int_0^1 \frac{\sinh(\alpha_L\xi)}{(1-\beta_L\xi)^2}\,d\xi \tag{38d}$$

where $\xi = (x + \delta_L)/\delta_L$ is an integration variable. In this way, as pointed out by Sistat et al.,[4] the impedance of a DBL presents three contributions: Z_{dL} is due to the variation in electric potential by a change in concentration profile; Z_{mL} is due to the variation in electric potential by a change in electric current when assuming the concentration profile does not change; and Z_{cL} is due to the variation in electric potential by a change in concentration profile produced by an electric current. It is worth noting that the conductive impedance does not have an analytical solution and must be numerically obtained,[4] but its limits at the lowest and highest frequencies are

$$\lim_{\omega\to 0} Z_{cL} = \frac{\delta_L t_{3L}}{z_3^2 D_{3S} c^L}\left[\frac{\ln(1-\beta_L)}{\beta_L} + \frac{1}{1-\beta_L}\right] \tag{39a}$$

$$\lim_{\omega\to\infty} Z_{cL} = 0 \tag{39b}$$

If we calculate the limits of the impedance of the left DBL, Z_L, at the lowest and the highest frequencies, we find that the geometric resistance of the left DBL, R_{acL}, is given by:

$$R_{acL} = \lim_{\omega\to\infty} Z_L = -\frac{\delta_L t_{3L}}{z_3^2 D_{3S} c^L}\frac{\ln(1-\beta_L)}{\beta_L} \tag{40a}$$

and the dc resistance of the left DBL, R_{DCL}, is

$$R_{DCL} = \lim_{\omega\to 0} Z_L = \left(\frac{1}{z_1} - \frac{1}{z_3}\right)\frac{1}{I_L(1-\beta_L)} \tag{40b}$$

In this way, by assuming that the frequency dependence of the conduction impedance is similar to that of the diffusion impedance,[4,7,8] the impedance of the left DBL can be written as

$$Z_L = R_{acL} + (R_{DCL} - R_{acL})\frac{\tanh\alpha_L}{\alpha_L} \tag{40c}$$

Now, by using the following boundary conditions

$$c_0(x = d + \delta_R) = 0 \tag{41a}$$

$$\left(\frac{dc_0}{dx}\right)_{x=d} = -\frac{I_0 c^R}{I_R\delta_R} \tag{41b}$$

the general solution of eq 33b in the right DBL is

$$c_0(x) = -\frac{I_0 c^R}{I_R\alpha_R}\frac{\sinh\left(\alpha_R\frac{x-d-\delta_R}{\delta_R}\right)}{\cosh\alpha_R} \tag{41c}$$

where

$$\alpha_R = \delta_R\sqrt{\frac{j\omega}{D_{SR}}} = \sqrt{j\omega\Lambda_R} \tag{41d}$$

Now, the ac component of the electric field in the right DBL, E_{R0}, is

$$E_{R0} = \frac{D_{3S} - \gamma_R D_{1S} - (1-\gamma_R)D_{2S}}{z_3 D_{3S}} t_{3R}\,\frac{d}{dx}\left(\frac{c_0}{c_{DC}}\right) + \frac{t_{3R} I_0}{z_3^2 D_{3S} c_{DC}} - \frac{t_{3R} I_{DC}}{z_3^2 D_{3S}}\frac{c_0}{c_{DC}^2} \tag{42a}$$

the electric potential difference in the neutral zone of the right DBL is

$$\phi_0^R = \int_d^{d+\delta_R} E_{R0}\,dx \tag{42b}$$

while the Donnan potential difference for counterions with identical valence at the right interface is

$$\phi_0^{dR} = -\frac{1}{z_1}\frac{c_0(x=d)}{c_{DC}(x=d)} = \frac{1}{z_1}\frac{I_0}{I_R(1+\beta_R)}\frac{\tanh\alpha_R}{\alpha_R} \tag{42c}$$

From the integration of eq 41b, one obtains that the impedance of the right DBL is

$$Z_R = \frac{\phi_0^R + \phi_0^{dR}}{I_0} = Z_{dR} + Z_{mR} + Z_{cR} \tag{43a}$$

where the diffusion impedance, Z_{dR}, is

$$Z_{dR} = \left(\frac{1}{z_1} - \frac{D_{3S} - \gamma_R D_{1S} - (1-\gamma_R)D_{2S}}{z_3 D_{3S}} t_{3R}\right)\frac{1}{I_R(1+\beta_R)}\frac{\tanh\alpha_R}{\alpha_R} \tag{43b}$$

the ohmic impedance, Z_{mR}, is

$$Z_{mR} = \frac{\delta_R t_{3R}}{z_3^2 D_{3S} c^R}\frac{\ln(1+\beta_R)}{\beta_R} \tag{43c}$$

and the impedance of conduction, Z_{cR}, is

$$Z_{cR} = \frac{t_{3R}\delta_R\beta_R}{z_3^2 D_{3S} c^R}\frac{1}{\alpha_R\cosh\alpha_R}\int_{-1}^0 \frac{\sinh(\alpha_R\xi)}{(1-\beta_R\xi)^2}\,d\xi \tag{43d}$$

where $\xi = (x - d - \delta_R)/\delta_R$ is the integration variable. Now, the limits of the conduction impedance of the right DBL at the lowest and highest frequencies are

dx.doi.org/10.1021/jp4108238 | J. Phys. Chem. C 2014, 118, 2539−2553

$$\lim_{\omega\to 0} Z_{cR} = -\frac{\delta_R t_{3R}}{z_3^2 D_{3S} c^R}\left[\frac{\ln(1+\beta_R)}{\beta_R} - \frac{1}{1+\beta_R}\right] \quad (44a)$$

$$\lim_{\omega\to \infty} Z_{cR} = 0 \quad (44b)$$

From the evaluation of the limits of the impedance of the right DBL at the lowest and highest frequencies, we find that the geometric resistance of the right DBL, R_{acR}, is given by

$$R_{acR} = \lim_{\omega\to\infty} Z_R = \frac{\delta_R t_{3R}}{z_3^2 D_{3S} c^R}\frac{\ln(1+\beta_R)}{\beta_R} \quad (45a)$$

and the dc resistance of the right DBL, R_{DCR}, is

$$R_{DCR} = \lim_{\omega\to 0} Z_R = \left(\frac{1}{z_1} - \frac{1}{z_3}\right)\frac{1}{I_R(1+\beta_R)} \quad (45b)$$

In this way, by assuming that the frequency dependence of the conductive impedance is similar to that of the diffusion impedance, the impedance of the right DBL can be written as

$$Z_R = R_{acR} + (R_{DCR} - R_{acR})\frac{\tanh \alpha_R}{\alpha_R} \quad (45c)$$

Finally, the electric potential difference through the membrane is

$$\phi_0^m = \int_0^d E_{m0}\, dx = R_M I_0 \quad (46)$$

Now, because we ignore the displacement current in the low-frequency range, the impedance Z_W can be obtained from the following equation:

$$Z_W = \frac{\phi_0^L + \phi_0^m + \phi_0^R}{I_0} = Z_L + R_M + Z_R \quad (47a)$$

In this way, the low-frequency diffusion impedance of the total ion-exchange membrane system, Z_W, can be written as:

$$Z_W = R_{ac} + (R_{DCL} - R_{acL})\frac{tanh\ \alpha_L}{\alpha_L} + (R_{DCR} - R_{acR})\frac{tanh\ \alpha_R}{\alpha_R} \quad (47b)$$

where

$$R_{ac} = R_M + R_{acL} + R_{acR} \quad (47c)$$

and the dc resistance of the system at the limit of the lowest frequencies is

$$R_{DC} = \lim_{\omega\to 0} Z_W = \left(\frac{1}{z_1} - \frac{1}{z_3}\right)\left(\frac{1}{I_L(1-\beta_L)} + \frac{1}{I_R(1+\beta_R)}\right) + R_M = R_{DCL} + R_{DCR} + R_M \quad (47d)$$

which agrees with eq 33a obtained from the steady-state analysis.

It must be taken into account that the low-frequency impedance is the superposition of the Warburg impedances corresponding to the left and right DBLs, and the characteristics frequencies are

$$f_{dL} = \frac{2.54}{2\pi\Lambda_L} \quad (48a)$$

and

$$f_{dR} = \frac{2.54}{2\pi\Lambda_R} \quad (48b)$$

It is worth noting that the low-frequency impedance of an ion-exchange membrane system can be considered as that of a single electric circuit constituted by the series association of five elements: the ohmic resistances of the left and right DBLs, the membrane resistance, and the two Warburg elements corresponding to the left and right DBLs.

3.3.2. High Frequency. In the high-frequency range, one can assume $c_0 = 0$ along the system. Then, by taking into account eqs 4 and 7a, one obtains by integration of eq 18 the following expressions:

$$I_0 = \frac{\phi_0^L}{R_{acL}} + j\omega\varepsilon\frac{\phi_0^L}{\delta_L} = \frac{\phi_0^m}{R_M} + j\omega\varepsilon\frac{\phi_0^m}{d} = \frac{\phi_0^R}{R_{acR}} + j\omega\varepsilon\frac{\phi_0^R}{\delta_R} \quad (49a)$$

Because the high-frequency or geometric impedance is given by

$$Z_g = \frac{\phi_0^L + \phi_0^m + \phi_0^R}{I_0} \quad (49b)$$

one finds the following expression:

$$Z_g = \frac{R_{acL}}{1 + j\omega R_{acL} C_{gL}} + \frac{R_M}{1 + j\omega R_M C_{gM}} + \frac{R_{acR}}{1 + j\omega R_{acR} C_{gR}} \quad (49c)$$

where the geometric capacitances are

$$C_{gL} = \frac{\varepsilon}{\delta_L} \quad (50a)$$

$$C_{gM} = \frac{\varepsilon}{d} \quad (50b)$$

$$C_{gR} = \frac{\varepsilon}{\delta_R} \quad (50c)$$

In this way, this geometric impedance is the superposition of the three simple geometric impedances of the left DBL, membrane, and right DBL, the characteristic frequencies being

$$f_{gL} = \frac{1}{2\pi R_{acL} C_{gL}} \quad (51a)$$

$$f_{gM} = \frac{1}{2\pi R_{acM} C_{gM}} \quad (51b)$$

$$f_{gR} = \frac{1}{2\pi R_{acR} C_{gR}} \quad (51c)$$

It must be noted that the high-frequency impedance corresponds to that of an electric circuit constituted by the series association of three single RC parallel branches. Moreover, it must be also noted that the capacitance of the diffuse double layer, such as included into the classical Randles circuit describing the impedance of the mass- and charge-transfer processes in an electrochemical interface,[5] has been neglected in our study. In the case of a ternary electrolyte, the diffuse double-layer capacitance at the left, C_{dlL}, and the right interfaces, C_{dlR}, are given by

$$C_{dlL} = \sqrt{\varepsilon(z_1^2 c_1^L + z_2^2 c_2^L + z_3^2 c_3^L)} \quad (52a)$$

$$C_{dlR} = \sqrt{\varepsilon(z_1^2 c_1^R + z_2^2 c_2^R + z_3^2 c_3^R)} \quad (52b)$$

In the Randles circuit, each one of them appears connected in parallel with the Warburg impedance of the corresponding DBL.

dx.doi.org/10.1021/jp4108238 | J. Phys. Chem. C 2014, 118, 2539−2553

However, we have checked that they exert a very poor influence because there is no charge-transfer resistance in the interfaces and the length of the systems will be considered to be much greater than the Debye length.[54]

4. RESULTS AND DISCUSSION

In this paper, the numerical results are obtained by using the network simulation method, which is briefly described in Appendix B, and they are presented for ion-exchange membranes placed between two solutions varying the chemical composition, γ_L and γ_R, the co-ion concentration, c^L and c^R, and the direct component of the electric current, I_{DC}. In the considered system, the counterions present identical values for the charge number, $z_1 = z_2 = 1$, and the following other parameters: $z_3 = -1$, $X = 10$, $d = 1000$, $\delta_L = \delta_R = 1000$, $\varepsilon = 1$, $D_{1S} = 1000$, $D_{2S} = 1500$, $D_{3S} = 1500$, $D_{1M} = 100$, $D_{2M} = 150$, and $D_{3M} = 150$. This system could correspond to a membrane immersed in a mixture of NaCl and KCl. The ionic diffusion coefficients in the membrane have been chosen as a tenth of those in the solutions for the sake of simplicity. In particular, this choice involves that the ratio of the diffusion coefficients of the ions in the membrane takes a value that is the same as that in the solutions.

4.1. Effect of Changing the Chemical Composition in an Unbiased Symmetric System. First, we will study the electrochemical impedance of the ion-exchange membrane system above-described when the membrane is placed between two symmetric solutions with identical chemical composition, $\gamma_L = \gamma_R = \gamma$, and salt concentrations $c^L = c^R = 0.1$ for $I_{DC} = 0$ and different values of γ. This arrangement is typical in experimental studies on the electrochemical properties of ion-exchange membranes used in electromembrane processes based on conventional electrodialysis with multi-ionic electrolytes.[55−58] Figure 1 gives the complex-plane impedance plots for three

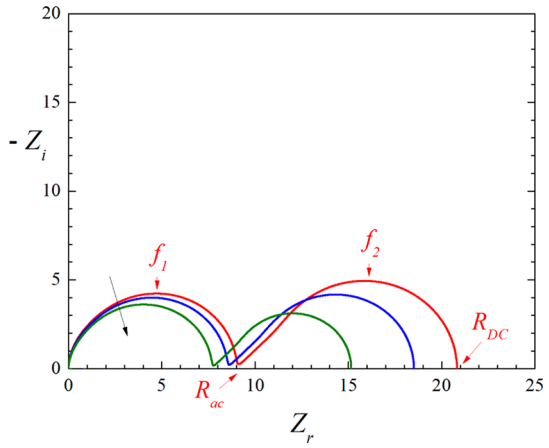

Figure 1. Complex-plane impedance plots for an ion-exchange membrane system with $\gamma_L = \gamma_R = \gamma$ and $c^L = c^R = 0.1$, for $I_{DC} = 0$ and different values of γ, namely, $\gamma = 0.25$, 0.75, and 1. The arrow indicates decreasing γ values.

values of γ, namely, $\gamma = 0.25$, 0.75, and 1. In these figure, $-Z_i(\omega)$ is plotted against $Z_r(\omega)$ with the angular frequency, ω, as a parameter increasing from the right to the left of the plot (Nyquist-type plot). In accord with eqs 8−10, the value $\gamma = 1$ corresponds to a binary system with the ions 1 and 2. Then, whatever the value of γ may be, the impedance plots show the main properties of the experimental plots obtained in ion-exchange membrane systems with binary electrolytes.[59−62] Each plot shows two regions: a geometric arc at high frequencies in the left of the plot and a diffusion arc at low frequencies in the right of the plot. In these plots shown in Figure 1, it is clearly observed that the geometric arc is like a distorted semicircle because half of its width is greater than its height. In fact, each term in eq 49c leads to a semicircle in the Nyquist-type impedance plot. In this way, each geometric arc in Figure 1 can be considered a distorted semicircle which comes from the sum of the geometric semicircles of the left solution, membrane, and right solution. On the other hand, each diffusion arc is a Warburg-type impedance[63−67] because it presents a 45° slope straight line at high frequencies and a semicircle at low frequencies.

From a given Nyquist-type plot, one can easily obtain and tabulate the following parameters:

- The dc resistance of the system, $R_{DC} = Z_r\,(f = 0)$, i.e., the real part of the impedance at the limit of zero frequency.
- The ohmic resistance of the system, i.e., the real part of the impedance at the intersection point between the geometric and diffusion arcs, R_{ac}. This parameter is obtained from the relative minimum value of the imaginary part of the impedance with a minus sign at low frequencies.
- The characteristic frequency of the diffusion arc, f_2, and the imaginary part of the impedance at this frequency, $Z_{i2} = Z_i(f_2)$. These values are obtained from the relative maximum value of the imaginary part of the impedance with a minus sign at low frequencies.
- The characteristic frequency of the geometric arc, f_1, and the imaginary part of the impedance at this frequency, $Z_{i1} = Z_i(f_1)$. These values are obtained from the relative maximum value of the imaginary part of the impedance with a minus sign at high frequencies.

In Table 1, the numerical results for the cited parameters are compared with those of the solutions obtained from the approximate expressions derived in Ideal Ion-Exchange Membrane Systems for ideal ion-exchange membranes with $I_{DC} = 0$ and different values of γ, namely, $\gamma = 1$, 0.75, and 0.25. The numerical results are in good agreement with those obtained from the approximate analytical expressions: eq 47d for R_{DC}, eq 47c for R_{ac}, eq 47b for f_2 and Z_{i2}, and eq 49c for f_1 and Z_{i1}. From eq 16, it is clear that a decrease in the value of γ leads to a decrease in the concentration of ion 1 and to an increase in the concentration of ion 2, this later being the ion with the greatest value of the diffusion coefficient in the system. In this way, a decrease in the value of γ leads to an increase in the conductivity of the DBLs (the denominator of the ionic transport numbers). As expected, from the results shown in Figure 1 and Table 1 it can be seen that the values of R_{ac} and R_{DC} decrease while the value of

Table 1. Numerical and Analytical Results for the Characteristics Parameters Used in the Interpretation of the Impedance Plots of Ion-Exchange Membrane Systems with $\gamma_L = \gamma_R = \gamma$, $c^L = c^R = 0.1$, for $I_{DC} = 0$ and Different Values of γ

	$\gamma = 1$		$\gamma = 0.75$		$\gamma = 0.25$	
	num	ideal	num	ideal	num	ideal
R_{DC}	20.82	21.00	18.51	18.66	15.15	15.27
$f_2 \times 10^4$	4.84	4.85	5.19	5.20	5.79	5.81
$-Z_{i2}$	4.95	5.01	4.18	4.24	3.13	3.17
R_{ac}	9.13	9.00	8.62	8.51	7.77	7.68
f_1	42.07	41.99	43.75	43.82	47.64	47.61
$-Z_{i1}$	4.24	4.24	4.01	4.01	3.62	3.63

dx.doi.org/10.1021/jp4108238 | J. Phys. Chem. C 2014, 118, 2539−2553

f_1 increases as γ decreases. Moreover, because the electrolyte diffusion coefficient obtained from eq 20 increases as the value of γ decreases, the characteristic frequency of the diffusion arc, f_2, increases as the value of γ decreases, as it can beseen in Table 1. It is worth highlighting that other authors[9,15] consider a third characteristic frequency in the system, which is associated with the frequency corresponding to the value obtained for the ohmic resistance, R_{ac}, at the intersection point of the geometric and diffusion arcs. However, this frequency is of the order of the geometric average of f_1 and f_2, $(f_1 f_2)^{1/2}$, and it is not explicitly considered in this work.

4.2. Effect of the dc Current in a Symmetric System. Now, we will study the electrochemical impedance of the ion-exchange membrane system above-described when the membrane is placed between two symmetric solutions with identical chemical composition, $\gamma_L = \gamma_R = \gamma = 0.5$, and salt concentrations, $c^L = c^R = 0.1$, for different values of the dc current, I_{DC}. To choose the appropriate values of the dc component of the electric current, previously we have obtained and represented in Figure 2

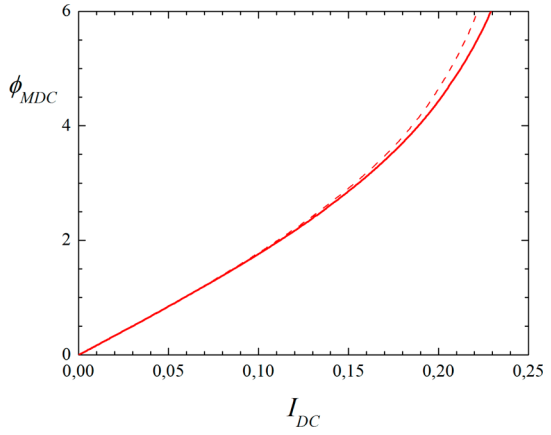

Figure 2. Steady-state voltage−current characteristic for an ion-exchange membrane system with $\gamma_L = \gamma_R = \gamma = 0.5$ and $c^L = c^R = 0.1$. The curve corresponding to the ideal system given by eq 53a is represented by a dotted line.

the steady-state voltage−current characteristic of the system. In this figure, the curve corresponding to the ideal system has also been represented by means of a dotted line. In this case, from eq 34c, one can obtain that this curve obeys the following simplified relation:

$$\phi_{MDC} = 2\ln\left(1 + \frac{I_{DC}}{I_R}\right) - 2\ln\left(1 - \frac{I_{DC}}{I_L}\right) + R_M I_{DC} \tag{53a}$$

where the resistance of the membrane, R_M, is given by

$$R_M = \frac{2d}{(D_{1M} + D_{2M})X} \tag{53b}$$

and the values of the limiting electric currents are $I_L = I_R = 0.25$. The numerical and analytical results are in good agreement except for the highest values of the electric current because of the nonideal behavior of the chosen system. In Figure 2 it can be appreciated that the slope of the steady-state voltage−current curve obtained from the numerical simulation of the Nernst−Planck and Poisson equations is smaller than that corresponding to an ideal ion-exchange membrane system.

Figure 3 shows the Nyquist plots for the impedance of the ion-exchange membrane system for different values of the dc

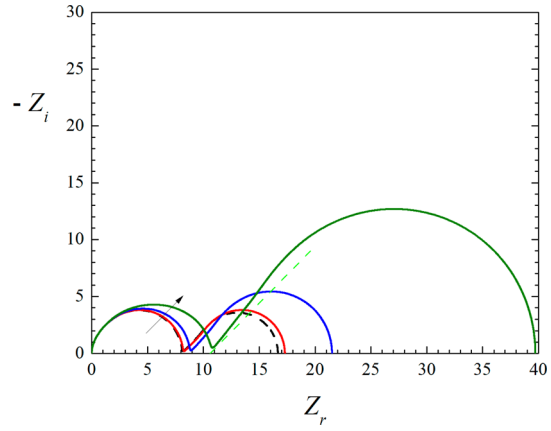

Figure 3. Complex-plane impedance plots for an ion-exchange membrane system with $\gamma_L = \gamma_R = \gamma = 0.5$ and $c^L = c^R = 0.1$, for different values of I_{DC}, namely, $I_{DC} = 0$, 0.05, 0.125, and 0.2. The arrow indicates increasing values of I_{DC}.

component of the electric current, namely, $I_{DC} = 0$, 0.05, 0.125, and 0.2. A dotted straight line with a slope of 45° is shown in this figure in order to compare the impedance obtained for $I_{DC} = 0.2$. These plots present the two characteristic arcs of the impedance of ion-exchange membrane systems. In Table 2, the numerical results for the characteristic parameters used in the interpretation of the Nyquist plots are compared with the solutions obtained from the expressions derived in Ideal Ion-Exchange Membrane Systems for ideal membranes. When a positive electric current passes through the system, the ionic concentrations decrease in the left DBL and they increase in the right DBL. Therefore, the conductivity of the depleted DBL strongly decreases as the value of I_{DC} increases. As expected, from the results presented in Figure 3 and Table 2 it can be observed that R_{ac} and R_{DC} increase while f_1 decreases as I_{DC} increases. On the other hand, it can be seen in Table 2 that the characteristic frequency of the diffusion arc, f_2, is not a function of the electric current dc. This theoretical result is a consequence of the independence of the dc current on the salt diffusion coefficient. However, this behavior is very difficult to experimentally reproduce because the thickness of the DBL depends on the dc component of the electric current because of the convection in the experimental stacks.[68−71] From Table 2 it can be seen that the numerical results are in good agreement with those obtained from the approximate analytical expressions in the high-frequency range. Moreover, there is an excellent agreement for the lowest values of the dc electric current in the low-frequency range. However, the results slightly differ for the highest values of the dc current in the low-frequency range. First, in Table 2 it can be appreciated that the numerical value of R_{DC} is higher than that obtained from the ideal system. This behavior is due to the differences found in the slopes of the steady-state voltage−current characteristics, as can be observed in Figure 2. Second, in Figure 3 it can be seen that the diffusion arc for $I_{DC} = 0.2$, which corresponds to 80% of the limiting current in the depleted DBL, slightly differs from that of the Warburg impedance. This arc, shown in Figure 3, exhibits a straight line at the highest frequencies, but the slope is higher than 45°. This behavior has already been observed in binary systems,[7,8] and it is due to the contribution of the conductive impedance. In Figure 4, the Nyquist plots of the low-frequency

dx.doi.org/10.1021/jp4108238 | J. Phys. Chem. C 2014, 118, 2539−2553

Table 2. Numerical and Analytical Results for the Characteristics Parameters Used in the Interpretation of the Impedance Plots of Ion-Exchange Membrane Systems with $\gamma_L = \gamma_R = \gamma = 0.5$, $c^L = c^R = 0.1$, and Different Values of I_{DC}

	$I_{DC} = 0$		$I_{DC} = 0.05$		$I_{DC} = 0.125$		$I_{DC} = 0.2$	
	num	ideal	num	ideal	num	ideal	num	ideal
R_{DC}	16.67	16.80	17.29	17.47	21.51	22.13	39.71	45.24
$f_2 \times 10^4$	5.50	5.51	5.50	5.51	5.50	5.51	5.50	5.51
$-Z_{i2}$	3.59	3.64	3.83	3.88	5.45	5.57	12.72	14.38
R_{ac}	8.17	8.07	8.27	8.17	8.89	8.79	10.81	10.79
f_1	45.71	45.71	44.87	44.87	39.72	39.81	28.05	27.04
$-Z_{i1}$	3.80	3.81	3.83	3.84	3.95	4.02	4.30	4.68

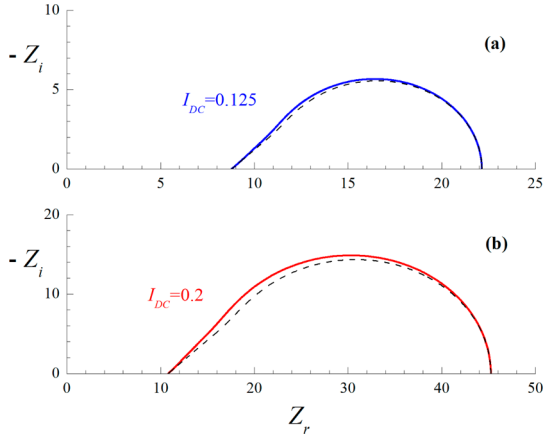

Figure 4. Complex-plane low-frequency impedance plots for an ion-exchange membrane system with $\gamma_L = \gamma_R = \gamma = 0.5$, $c^L = c^R = 0.1$, and $I_{DC} = 0.125$ (a) and 0.2 (b). The solid lines correspond to the impedance with a numerical evaluation of the conductive contribution, while the dotted lines correspond to the Warburg approximate impedance.

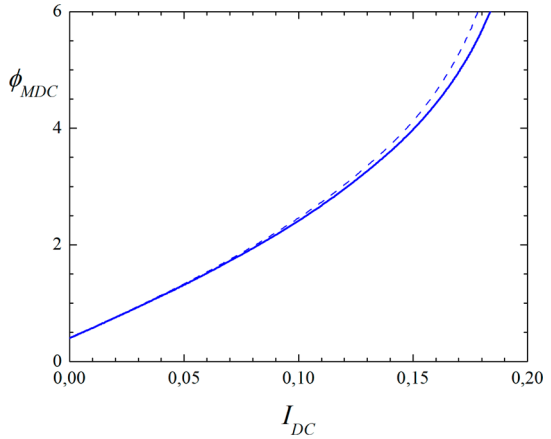

Figure 5. Steady-state voltage−current characteristic for an ion-exchange membrane system under bi-ionic conditions with $\gamma_L = 1$, $\gamma_R = 0$, and $c^L = c^R = 0.1$. The curve corresponding to the ideal system given by eq 54a is represented by a dotted line.

impedance of the system, Z_W, have been represented by using eq 47b, which corresponds to a Warburg-type impedance, and that given by eq 47a, where the conductive contributions to the impedance included in Z_L (eq 38a) and Z_R (eq 43a) have been numerically evaluated from eqs 38d and 43d, respectively, for the dc electric currents $I_{DC} = 0.125$ and 0.2. The results shown in this figure confirm that the distortion in the diffusion arc of Figure 4 is due to the conductive contribution to the impedance; this effect is more significant for dc components of the electric current close to the limiting current of the system, $I_L = 0.25$.

4.3. System under Bi-ionic Conditions. In this section, we will study the electrochemical impedance of an ion-exchange membrane system under bi-ionic conditions, i.e., when the membrane is placed between two solutions with identical salt concentration $c^L = c^R = 0.1$, but the counterion 1 is in the left solution, $\gamma_L = 1$, and the counterion 2 is in the right solution, $\gamma_R = 0$, for different values of the dc component of the electric current, I_{DC}. This arrangement is characteristic in the field of the ion-selective electrodes used as electrochemical sensors in those situations in which the counterion in the sample is different from that in the inlet solution.[72,73] Figure 5 shows the steady-state voltage−current characteristic of the system and a dotted line corresponding to that of the ideal system. From eq 32b, one can write the steady-state voltage−current curve in the ideal system in the following simplified way:

$$\phi_{MDC} = 2\ln\left(1 + \frac{I_{DC}}{I_R}\right) - 2\ln\left(1 - \frac{I_{DC}}{I_L}\right) + \phi_{BII} + R_M I_{DC} \tag{54a}$$

where the equilibrium bi-ionic electric potential, ϕ_{BII}, is given by[16]

$$\phi_{BII} = \ln\left(\frac{D_{2M}}{D_{1M}}\right) \tag{54b}$$

and the membrane resistance under bi-ionic conditions can be expressed as

$$R_M = \frac{d}{(D_{2M} - D_{1M})X}\ln\left(\frac{D_{2M}}{D_{1M}}\right) \tag{54c}$$

It must be noted that the measure of the equilibrium bi-ionic potential of a charged membrane is of great practical interest because it provides the ratio between the diffusion coefficients of the counterions inside the membrane. The numerical and analytical results are in good agreement except for the highest values of the electric current. In Figure 5 it can be appreciated that the slope of the steady-state voltage−current curve obtained from the numerical simulation of the transport equations including the diffuse double-layer effects is smaller than that corresponding to an ideal ion-exchange membrane system in the high-current region.

The Nyquist plots for the impedance of the system under bi-ionic conditions for different values of the dc component of the electric current in the underlimiting current regime, namely, $I_{DC} = 0$, 0.05, and 0.1, are shown in Figure 6. These plots present two arcs in a way similar to those obtained for the systems previously studied. In Table 3, the numerical results for characteristic parameters of the Nyquist plots are compared with the solutions obtained from the analytical expressions derived in Ideal Ion-

dx.doi.org/10.1021/jp4108238 | J. Phys. Chem. C 2014, 118, 2539−2553

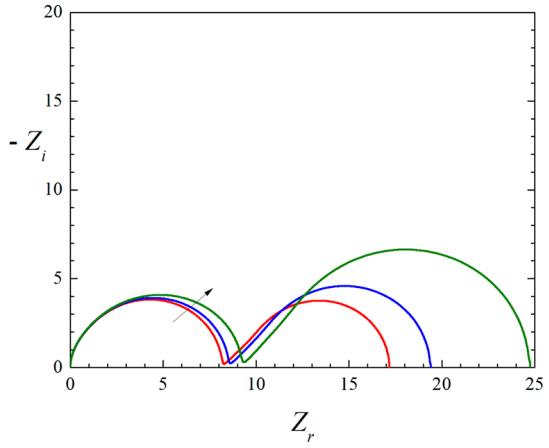

Figure 6. Complex-plane impedance plots for an ion-exchange membrane system under bi-ionic conditions with $\gamma_L = 1$, $\gamma_R = 0$, and $c^L = c^R = 0.1$, for different values of $I_{DC} = 0$, namely, $I_{DC} = 0, 0.05, 0.1$. The arrow indicates increasing values of I_{DC}.

Table 3. Numerical and Analytical Results for the Characteristics Parameters Used in the Interpretation of the Impedance Plots of Ion-Exchange Membrane Systems under Bi-ionic Conditions with $\gamma_L = 1$, $\gamma_R = 0$, $c^L = c^R = 0.1$, and Different Values of I_{DC}

	$I_{DC} = 0$		$I_{DC} = 0.05$		$I_{DC} = 0.1$	
	num	ideal	num	ideal	num	ideal
R_{DC}	17.16	17.48	19.40	19.86	24.74	25.81
$f_2 \times 10^4$	5.45	5.26	5.33	5.11	5.20	4.99
$-Z_{i2}$	3.77	3.87	4.59	4.72	6.65	6.90
R_{ac}	8.27	8.14	8.62	8.50	9.34	9.23
f_1	44.98	45.19	42.36	42.33	37.15	36.75
$-Z_{i1}$	3.83	3.83	3.92	3.93	4.09	4.16

Exchange Membrane Systems for ideal systems. These results are in excellent agreement. In the bi-ionic system, the electrolyte diffusion coefficients are different in the two DBLs, and the diffusion arc comes from the superposition of two Warburg arcs with different characteristic frequencies, $f_{dL} = 4.85 \times 10^{-4}$ and $f_{dR} = 6.06 \times 10^{-4}$, obtained from eqs 48a and 48b. If the direct electric current passing through the system is positive, the left DBL becomes depleted and its conductivity strongly decreases as the value of I_{DC} increases; this fact determines the main properties of the impedance plots. As expected, from the results presented in Figure 6 and Table 3, it can be observed that R_{ac} and R_{DC} increase while f_1 decreases as I_{DC} increases. The frequency f_2 slightly decreases as I_{DC} increases because the characteristic frequency of the left Warburg arc is smaller than that of the right.

4.4. System in Asymmetric Arrangements. Finally, we will study the impedance of the ion-exchange membrane system when the membrane is placed between two solutions with different salt concentration, $c^L = 1$ and $c^R = 0.1$, with the same chemical composition, $\gamma_L = \gamma_R = \gamma = 0.5$, for different values of I_{DC}. Because $c^L > c^R$, there is a salinity gradient which produces a steady-state electric current through the system. In order to appropriately justify the chosen values of the dc currents, previously we have analyzed the steady-state voltage−current characteristic of the system in Figure 7 together with the curve corresponding to the ideal system. From eq 34c, one obtains that this curve is given by

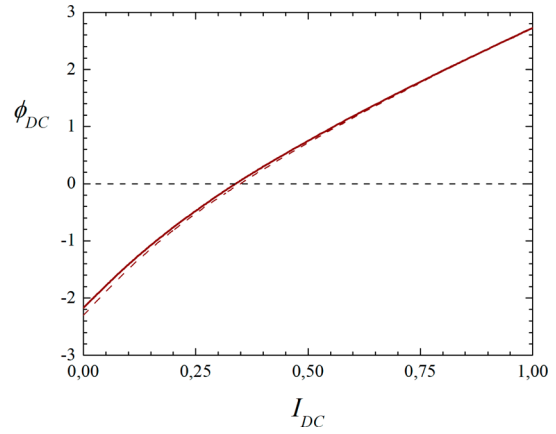

Figure 7. Steady-state voltage−current characteristic for an ion-exchange membrane system in an asymmetric arrangement with $\gamma_L = \gamma_R = \gamma = 0.5$, $c^L = 1$, and $c^R = 0.1$. The dotted line corresponds to that of an ideal system given by eq 55a.

$$\phi_{MDC} = 2\ln\left(1 + \frac{I_{DC}}{I_R}\right) - 2\ln\left(1 - \frac{I_{DC}}{I_L}\right) + \phi_{OCV} + R_M I_{DC} \quad (55a)$$

where the open circuit voltage, ϕ_{OCV}, is[74,75]

$$\phi_{OCV} = \ln\left(\frac{c^R}{c^L}\right) \quad (55b)$$

and the membrane resistance is given by eq 53b. The steady-state electric current leading to a zero electric potential is called short-circuit current, and it is approximately $I_{DC} = 0.35$ in our system, as can be inferred from Figure 7. It is well-known that a reverse electrodialysis stack supplies the maximum electric power when the electric current is a half of the short-circuit current.[74−76] The numerical and analytical results shown in Figure 7 are in good agreement, although it can be appreciated that the equilibrium voltage of the system, i.e., that corresponding to $I_{DC} = 0$, slightly differs from the open circuit voltage because of the nonideal behavior of the system. It must be noted that Figure 7 shows only the underlimiting current region because the limiting current of the system corresponds to that of the concentrated bath, $I_L = 2.5$.

Figure 8 shows the Nyquist plots for the impedance of the ion-exchange membrane system for different values of the dc component of the electric current in the underlimiting current regime, namely, $I_{DC} = 0$, 0.075, and 0.15. In Table 4, the numerical results for the characteristic parameters used in the interpretation of the Nyquist plots are compared with the solutions obtained from the approximate expressions derived in Ideal Ion-Exchange Membrane Systems for ideal membranes, and it can appreciated that they are in good agreement. In Figure 8, it can be observed that the high-frequency geometric arcs are strongly distorted. This behavior is due to the different values taken by the characteristic frequencies of the single geometric arcs corresponding to the left and right DBLs. For example, from eqs 51a−51c, one obtains $f_{gL} = 437.7$ and $f_{gR} = 43.8$ for $I_{DC} = 0$. Because the ionic concentration in the left bath is 10 times that of the right, the properties of the impedance plots are mainly determined by the right DBL. When a positive electric current passes through the system, the ionic concentrations increase in the right DBL, and the conductivity of this DBL strongly increases as the value of I_{DC} increases. As expected, from the

dx.doi.org/10.1021/jp4108238 | J. Phys. Chem. C 2014, 118, 2539−2553

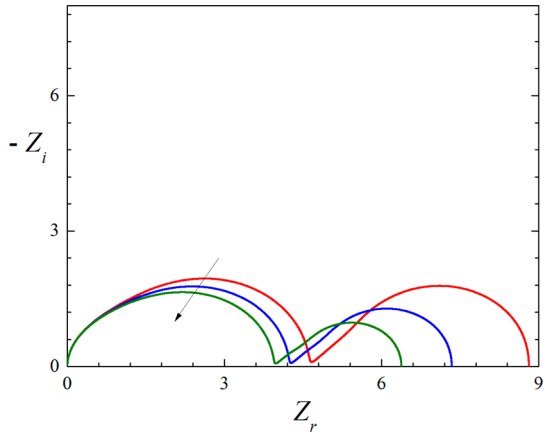

Figure 8. Complex-plane impedance plots for an ion-exchange membrane system in an asymmetric arrangement with $\gamma_L = \gamma_R = \gamma = 0.5$, $c^L = 1$, and $c^R = 0.1$, for different values of $I_{DC} = 0$, namely, $I_{DC} = 0$, 0.075, 0.15. The arrow indicates increasing values of I_{DC}.

Table 4. Numerical and Analytical Results for the Characteristics Parameters Used in the Interpretation of the Impedance Plots of Ion-Exchange Membrane Systems in an Asymmetric Arrangement with $\gamma_L = \gamma_R = \gamma = 0.5$, $c^L = 1$, $c^R = 0.1$, and different values of I_{DC}

	$I_{DC} = 0$		$I_{DC} = 0.05$		$I_{DC} = 0.1$	
	num	ideal	num	ideal	num	ideal
R_{DC}	8.81	9.60	7.34	7.78	6.38	6.65
$f_2 \times 10^4$	5.52	5.52	5.52	5.51	5.52	5.51
$-Z_{i2}$	1.79	2.00	1.29	1.43	0.97	1.10
R_{ac}	4.66	4.80	4.27	4.35	3.98	4.02
f_1	52.00	49.00	60.53	57.92	69.02	66.77
$-Z_{i1}$	1.95	2.03	1.78	1.84	1.65	1.70

results presented in Figure 8 and Table 4, it can be observed that R_{ac} and R_{DC} decrease while f_1 increases as I_{DC} increases. On the other hand, the frequency f_2 is not a function of the dc component of the electric current, I_{DC}, because the Warburg factor (the argument of the hyperbolic tangent function) is identical in the two DBLs.

4. CONCLUSIONS

A theoretical study of the electrochemical impedance of a system constituted by an ion-exchange membrane and two diffusion boundary layers on both sides of the membrane, immersed in ternary electrolyte solutions with two counterions, has been presented. An approximate analytical expression has been arranged for the impedance of an ideal ion-exchange membrane system for counterions with the same charge number on the basis of the Nernst–Planck–Donnan equations under electroneutrality. The electrochemical impedance for different values of the direct electric current of ion-exchange membrane systems with univalent ions has been numerically obtained from the Nernst–Planck and Poisson equations. The results have been compared with the approximate analytical expressions in different arrangements of practical interest, including conventional electrodialysis, bi-ionic conditions, and reverse electrodialysis.

The Nyquist plots of the electrochemical impedance of ion-exchange membranes in ternary electrolyte solutions with two counterions present two arcs, in accord with the approximate analytical solutions, consisting of a high-frequency geometric impedance and the low-frequency Warburg diffusion impedance such as occurs in similar systems with binary electrolytes. It can be established that the Warburg diffusion impedance appropriately models the low-frequency impedance of an ion-exchange membrane in ternary electrolyte solutions except for the highest values of the dc component of the electric current, close to the limiting current, because of the significant contribution of the conductive impedance. Moreover, the generalized expressions for ternary electrolyte solutions with two counterions of the ionic transport numbers, electrolyte diffusion coefficients, limiting electric currents, and resistance of the membrane allow us to interpret the impedance plots on the basis of the single electric elements known for binary electrolytes.

APPENDIX A

In this work, the survey is presented by using dimensionless variables. They are obtained by dividing the variable by the following scaling factors:

- Molar concentration and fixed-charge concentration (mol m^{-3}): c_a
- Diffusion coefficient (m^2 s^{-1}): D_a
- Position and length (m): λ
- Time (s): λ^2/D_a
- Ionic flux (mol m^{-2} s^{-1}): $(D_a c_a)/\lambda$
- Electric potential (V): $(RT)/F$
- Electric field (V m^{-1}): $(RT)/(F\lambda)$
- Electric displacement (C m^{-2}): $Fc_a\lambda$
- Electric permittivity (C V^{-1} m^{-1}): $(F^2 c_a \lambda^2)/(RT)$
- Electric current (A m^{-2}): $(FD_a ca)/\lambda$
- Resistance (Ω m^2): $(RT\lambda)/(F^2 D_a c_a)$
- Capacitance (C V^{-1} m^{-2}): $(F^2 c_a \lambda)/(RT)$
- Frequency (s^{-1}): D_a/λ^2

The constants F, R, and T have their usual meanings: Faraday constant (C mol^{-1}), ideal gas constant (J K^{-1} mol^{-1}), and absolute temperature (K), respectively. The parameters λ, D_a, and c_a are scaling factors with the dimensions of length, diffusion coefficient, and molar concentration, respectively. These three variables are chosen as characteristic values of the system studied. In particular, if one takes $\varepsilon = 1$, the length λ given by

$$\lambda = \sqrt{\frac{\varepsilon_r \varepsilon_0 RT}{F^2 c_a}}$$

where ε_r is the relative dielectric constant and ε_0 the electric permittivity of the vacuum, can be considered the Debye length in the system. Using typical values of the diffusion coefficient and the ionic concentration in the solutions such 10^{-9} m^2 s^{-1} and 0.1 M,[4] one obtains $D_a = 10^{-12}$ m^2 s^{-1} and $c_a = 1$ M. Then, for $\varepsilon_r = 80$ and $T = 300$ K, the Debye length of the system, λ, is approximately 2 nm. Thus, 1 unit of frequency, electric potential, electric current, resistance, and capacitance is 250 kHz, 25 mV, 1 A cm^{-2}, 0.13 Ω cm^2, and 15 μF cm^{-2}, respectively.

APPENDIX B

The network simulation method basically consists of modeling a physical or chemical process by means of a graphical representation analogous to circuit electrical diagrams, which is analyzed by means of an electric circuit simulation program. Highly developed, commercially available software for circuit analysis (PSpice from Cadence Design Systems) can thus be employed to obtain the dynamic behavior of a system without having to deal with the solution of the governing differential equations.[37]

dx.doi.org/10.1021/jp4108238 | J. Phys. Chem. C 2014, 118, 2539–2553

The network model is obtained from a viewpoint similar to that of a finite difference scheme by dividing the physical region of interest, which we consider to have a unit cross-sectional area, into N volume elements or compartments of width δ_k (k = 1, ..., N) small enough for the spatial variations of the parameters within each compartment to be negligible.[37] The network model for the diffusion−migration process in a compartment of width δ_k, which is extended from $x_k - \delta_k/2$ to $x_k + \delta_k/2$, is shown in Figure B1, and a complete explanation of the general procedure

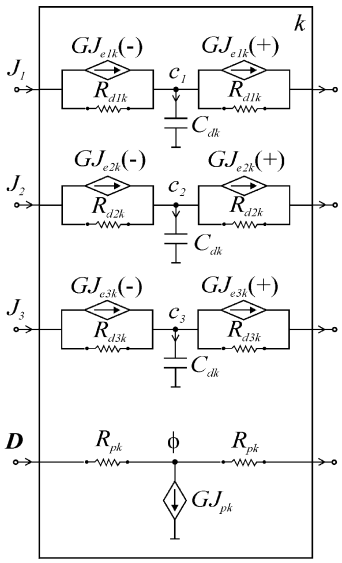

Figure B1. Network model for the electrodiffusion of a ternary electrolyte in a volume element.

to obtain it can be found elsewhere.[38,39] In this figure, the network elements are as follows: R_{dik} is the resistor representing the diffusion of ion i in the compartment k; $GJ_{eik}(\pm)$ is the voltage-controlled current source modeling the electrical contribution to the ionic flux, minus and plus signs meaning the flux entering and leaving the compartment k, respectively; C_{dk} is the capacitor representing the nonstationary effects of the electrodiffusion process in the compartment k; R_{pk} is the resistor modeling the constitutive equation of the medium; and GJ_{pk} is the voltage-controlled current source modeling the electric charge stores in the compartment k. The relation between those network elements and the parameters of the system is given by:

$$R_{dik} = \frac{\delta_k}{2D_{ip}} \tag{B1}$$

$$GJ_{eik}(\pm) = \pm\, D_{ip} z_i c_i\left(\xi_k \pm \frac{\delta_k}{2}\right)\frac{\phi(\xi_k) - \phi\left(\xi_k \pm \frac{\delta_k}{2}\right)}{\delta_k/2}, \quad i = 1, 2, 3 \tag{B2}$$

$$C_{dk} = \delta_k \tag{B3}$$

$$R_{pk} = \frac{\delta_k}{2\varepsilon} \tag{B4}$$

$$GJ_{pk} = -\,\delta_k[z_1c_1(\xi_k) + z_2c_2(\xi_k) + z_3c_3(\xi_k) - \theta(\xi_k)] \tag{B5}$$

For network modeling purposes, a number N of circuit elements like those in Figure B1 (k = 1, ..., N) with the appropriate values of the diffusion coefficients and the fixed-charge concentration must be connected in series to form a network model for the entire physical region undergoing an electrodiffusion process.

Figure B2 shows the network model for an ion-exchange membrane system. In this figure, the eight-terminal box consists

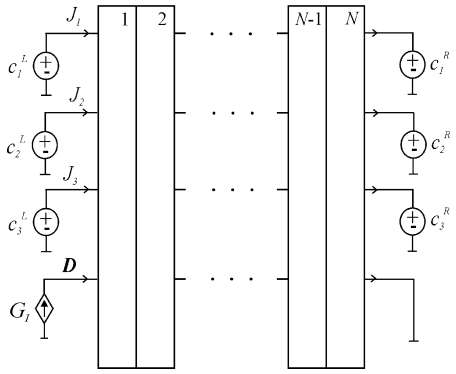

Figure B2. Network model for an ion-exchange membrane system. The eight-terminal box is obtained by the combination in series of N structures such us those shown in Figure B1.

of the combination in series of N elements such as those shown in Figure B1. In the network model of Figure B2, the concentrations of the ith species in the bathing solutions are represented by independent voltage sources of values c_i^L and c_i^R, which are obtained from eqs 8−10, while the external electric current perturbation, $I(\tau)$, is introduced from a controlled current source, G_I, by using eq 11a.

The spatial grid (N and δ_k) chosen considers the presence of two membrane−solution interfaces, two solution phases, and a membrane phase. Moreover, it takes into account that the different interfacial regions have a size of about 4λ in each phase.[45] This spatial grid is symmetrical about the interface in the two solution phases. In the left solution phase, we have chosen 100 compartments of width $(\delta_L - 10)/100$ from $x = -\delta$ to $x = -10$, 200 compartments of width 0.03 from $x = -10$ to $x = -4$, and 200 compartments of width 0.02 from $\xi = -4$ to $\xi = 0$. Moreover, the spatial grid is symmetrical about the middle point of the membrane, and we have chosen 200 compartments of width 0.02 from $x = 0$ to $x = 4$, 200 compartments of width 0.03 from $x = 4$ to $x = 10$, and 100 compartments of width $[(d/2) - 10]/100$ from $x = 10$ to $x = d/2$. In this way, N = 2000 compartments have been used: 500 for each solution phase and 1000 for the membrane.

Simulation of the network model shown in Figure B2 with the appropriate values for the parameters of the system into the PSpice program under small-signal ac conditions allows us to obtain the electrochemical impedance of ion-exchange membranes in ternary electrolyte solutions. At the beginning of the small-signal ac analysis, the dc bias point is calculated and the steady-state voltage−current characteristic of a system can be easily obtained. Actually, the main advantage of the network simulation method with respect to other numerical methods lies in the fact that it allows us to obtain not only the small-signal ac response but also the steady-state and transient responses, whatever the parameters of the system and the experimental conditions may be, on the basis of only a network model. The network models are of a quite complex nature because of the use of controlled current and voltage sources, but they can be used to represent the impedance of electrochemical systems by using

dx.doi.org/10.1021/jp4108238 | J. Phys. Chem. C 2014, 118, 2539−2553

electric elements distributed in space, such as those pointed out by Buck et al.[77] On the other hand, PSpice is a general purpose electric circuit simulation program, and it allows us to deal with the impedance of equivalent electric circuits described in terms of the Laplace variable, allowing the simulation of electric circuits containing both lumped and distributed frequency-dependent elements.

AUTHOR INFORMATION

Notes

The authors declare no competing financial interest.

REFERENCES

(1) Strathmann, H. Electrodialysis: A mature technology with a multitude of new applications. *Desalination* **2010**, *264*, 268−288.

(2) Logan, B. E.; Elimelech, M. Membrane-based processes for sustainable power generation using water. *Nature* **1012**, *488*, 313−319.

(3) Wang, W.; Luo, Q.; Li, B.; Wei, X.; Li, L.; Yang, Z. Recent progress in redox flow battery research and development. *Adv. Funct. Mater.* **2013**, *23*, 970−986.

(4) Sistat, P.; Kozmai, A.; Pismenskaya, N.; Larchet, C.; Pourcelly, G.; Nikonenko, V. Low-frequency impedance of an ion-exchange membrane system. *Electrochim. Acta* **2008**, *53*, 6380−6390.

(5) Nikonenko, V.; Kozmai, A. Electrical equivalent circuit of an ion-exchange membrane system. *Electrochim. Acta* **2011**, *56*, 1262−1269.

(6) Mareev, A.; Nikonenko, V. A numerical appoach to modeling impedance: Application to study a Warburg-type spectrum in a membrane system with diffusion coefficients depending on concentration. *Electrochim. Acta* **2012**, *81*, 268−274.

(7) Moya, A. A. Electric circuits modelling the low-frequency impedance of ideal ion-exchange membrane systems. *Electrochim. Acta* **2012**, *62*, 296−304.

(8) Moya, A. A. Harmonic analysis in ideal ion-exchange membrane systems. *Electrochim. Acta* **2013**, *90*, 1−11.

(9) Rubinstein, I.; Zaltzman, B.; Futerman, A.; Gitis, V.; Nikonenko, V. Reexamination of electrodiffusion time scales. *Phys. Rev. E* **2009**, *79* (021506), 1−6.

(10) Moya, A. A. Study of the electrochemical impedance and the linearity of the current−voltage relationship in inhomogeneous ion-exchange membranes. *Electrochim. Acta* **2010**, *55*, 2087−2092.

(11) Moya, A. A.; Moleón, J. A. Study of the electrical properties of bi-layer ion-exchange membrane systems. *J. Electroanal. Chem.* **2010**, *647*, 53−59.

(12) Moya, A. A. Influence of dc electric current on the electrochemical impedance of ion-exchange membrane systems. *Electrochim. Acta* **2011**, *56*, 3015−3022.

(13) Moya, A. A. Electrochemical impedance of ion-exchange membranes in asymmetric arrangements. *J. Electroanal. Chem.* **2011**, *660*, 153−162.

(14) Moya, A. A. Electrochemical impedance of ion-exchange systems with weakly charged membranes. *Ionics* **2013**, *19*, 1271−1283.

(15) Nandigana, V. V. R.; Aluru, N. R. Characterization of electrochemical properties of a micro-nanochannel integrated system using computational impedance spectroscopy (CIS). *Electrochim. Acta* **2013**, *105*, 514−523.

(16) Guirao, A.; Mafé, S.; Manzanares, J. A.; Ibañez, J. A. Biionic potential of charged membranes: Effects of the diffusion boundary layers. *J. Phys. Chem.* **1995**, *99*, 3387−3393.

(17) Dammak, L.; Larchet, C.; Auclair, B.; Manzanares, J. A.; Mafé, S. The influence of the salt concentration and the difusion boundary layers on the bi-ionic potetial. *J. Membr. Sci.* **1996**, *119*, 81−90.

(18) Dammak, L.; Larchet, C.; Auclair, B. Theoretical study of the bi-ionic potential and confrontation with experimental results. *J. Membr. Sci.* **1999**, *155*, 193−207.

(19) Danielsson, C.-O.; Dahlkild, A.; Velin, A.; Behm, M. A model for the enhanced water dissociation on monopolar membranes. *Electrochim. Acta* **2009**, *54*, 2983−2991.

(20) Andersen, M. B.; Soestbergen, M.; van Mani, A.; Bruus, H.; Biesheuvel, P. M.; Bazant, M. Z. Current-induced membrane discharge. *Phys. Rev. Lett.* **2012**, *109* (108301), 1−5.

(21) Mafé, S.; Manzanares, J. A.; Ramírez, P. Model for ion transport in bipolar membranes. *Phys. Rev. A* **1990**, *42*, 6245−6248.

(22) Kovalchuk, V. I.; Zholkovskij, E. K.; Aksenenko, E. V.; Gonzalez-Caballero, F.; Dukhin, S. S. Ionic transport across bipolar membrane and adjacent Nernst layers. *J. Membr. Sci.* **2006**, *284*, 255−266.

(23) Dickinson, E. J. F.; Freitag, L.; Compton, R. G. Dynamic theory of liquid junction potentials. *J. Phys. Chem. B* **2010**, *114*, 187−197.

(24) Ward, K. R.; Dickinson, E. J. F.; Compton, R. G. Dynamic theory of type 3 liquid junction potentials: Formation of multilayer liquid junctions. *J. Phys. Chem. B* **2010**, *114*, 4521−4528.

(25) Ward, K. R.; Dickinson, E. J. F.; Compton, R. G. Dynamic theory of membrane potentials. *J. Phys. Chem. B* **2010**, *114*, 10763−10773.

(26) van Soestbergen, M. Diffuse layer effects on the current in galvanic cells containing supporting electrolyte. *Electrochim. Acta* **2010**, *35*, 1848−1854.

(27) Danilov, D.; Notten, P. H. L. Li-ion electrolyte modeling: The impact of adding supportive salts. *J. Power Sources* **2009**, *189*, 303−308.

(28) Kucza, W.; Danielewski, M.; Lewenstam, A. EIS simulations for ion-selective site-based membranes by a numerical solution of the coupled Nernst-Planck-Poisson equations. *Electrochem. Commun.* **2006**, *8*, 416−420.

(29) Grysakowski, B.; Jasielec, J. J.; Wierzba, B.; Solkalski, T.; Lewentam, A.; Danielewski, M. Electrochemical impedance spectroscopy (EIS) of ion sensors direct modeling and inverse problem solving using the Nernst-Planck-Poisson (NPP) model and the HGS(FP) optimization strategy. *J. Electroanal. Chem.* **2011**, *662*, 143−149.

(30) Higa, M.; Tanioka, A.; Miyasaka, K. A study of ion permeation across a charged membrane in multicomponent ion systems as a function of membrane charge density. *J. Membr. Sci.* **1990**, *49*, 145−169.

(31) Manzanares, J. A.; Vergara, J.; Mafé, S.; Kontturi, K.; Viinikka, P. Potentiometric determination of transport numbers of ternary electrolyte systems in charged membranes. *J. Phys. Chem. B* **1998**, *102*, 1301−1307.

(32) Tasaka, M.; Kiyono, R.; Yoo, D.-S. Membrane potential across a high water content anion-exchange membrane separating two solutions with a common counterion but two different co-ions. *J. Phys. Chem. B* **1999**, *103*, 173−177.

(33) Fila, V.; Bouzek, K. A mathematical model of multiple ion transport across an ion-selective membrane under current load conditions. *J. Appl. Electrochem.* **2003**, *33*, 675−684.

(34) Lanteri, Y.; Szymczyk, A.; Fievet, P. Membrane potential in multi-ionic mixtures. *J. Phys. Chem. B* **2009**, *113*, 9197−9204.

(35) Geraldes, V.; Afonso, M. D. Limiting current density in the electrodialysis of multi-ionic solutions. *J. Membr. Sci.* **2010**, *360*, 499−508.

(36) Lakshminarayanaiah, N. *Equations of Membrane Biophysics*; Academic: New York, 1984.

(37) Bockris, J.O'M. ; Reddy, A. K. N. *Modern Electrochemistry*, 2nd ed.; Plenum Press: New York, 1998; Vol. *1*.

(38) Moleón, J. A.; Moya, A. A. Network simulation of the electrical response of ion-exchange membranes with fixed charge varying linearly with position. *J. Electroanal. Chem.* **2008**, *613*, 23−34.

(39) Moleón, J. A.; Moya, A. A. Transient electrical response of ion-exchange membranes with fixed-charge due to ion adsorption. A network simulation approach. *J. Electroanal. Chem.* **2009**, *633*, 306−313.

(40) Jamnik, J.; Maier, J. Treatment of the impedance of mixed condutors equivalent circuit model and explicit approximate solutions. *J. Electrochem. Soc.* **1999**, *146*, 4183−4188.

(41) Jamnik, J.; Maier, J. Generalised equivalent circuits for mass and charge transport: Chemical capacitance and its implications. *Phys. Chem. Chem. Phys.* **2001**, *3*, 1668−1678.

(42) Lai, W.; Haile, S. M. Impedance spectroscopy as a tool for chemical and electrochemical analysis of mixed conductors: A case study of ceria. *J. Am. Ceram. Soc.* **2005**, *88*, 2979−2997.

(43) Lai, W.; Ciucci, F. Small-signal apparent diffusion impedance of intercalation battery electrodes. *J. Electrochem. Soc.* **2011**, *158*, A115−A121.
(44) Ciucci, F.; Lai, W. Electrochemical impedance spectroscopy of phase trasition materials. *Electrochim. Acta* **2012**, *81*, 205−215.
(45) Manzanares, J. A.; Murphy, W. D.; Mafé, S.; Reiss, H. Numerical simulation of the nonequilibrium diffuse double layer in ion-exchange membranes. *J. Phys. Chem.* **1993**, *97*, 8524−8530.
(46) Moya, A. A.; Horno, J. Application of the network simulation method to ionic transport in ion-exchange membranes including diffuse double-layer effects. *J. Phys. Chem. B* **1999**, *103*, 10791−10799.
(47) Sokalski, T.; Lingenfelter, P.; Lewenstam, A. Numerical solution of the coupled Nernst−Planck and Poisson equations for liquid junction and ion selective membrane potentials. *J. Phys. Chem. B* **2003**, *107*, 2443−2452.
(48) Volgin, V. M.; Davydov, A. D. Ionic transport through ion-exchange and bipolar membranes. *J. Membr. Sci.* **2005**, *259*, 110−121.
(49) Morf, W. E.; Pretsch, E.; De Rooij, N. F. Computer simulation of ion-selective membrane electrodes and related systems by finite-difference procedures. *J. Electroanal. Chem.* **2007**, *602*, 43−54.
(50) Brumleve, T. R.; Buck, R. P. Numerical solution of the Nernst-Planck and Poisson equation system with applications to membrane electrochemistry and solid state physics. *J. Eleactroanal. Chem.* **1978**, *90*, 1−31.
(51) Barsoukov, E.; Macdonald, J. R. *Impedance Spectroscopy: Theory, Experiment and Applications*; Wiley: New York, 2005.
(52) Helfferich, F. *Ion Exchange*; McGraw-Hill: NY, 1962.
(53) Konturri, K.; Murtomäki, L.; Manzanares, J. A. *Ionic Transport Processes in Electrochemistry and Membrane Science*; Oxford University Press: New York, 2008.
(54) Brumleve, T. R.; Buck, R. P. Transmission line equivalent circuit models for electrochemical impedances. *J. Electroanal. Chem.* **1981**, *126*, 73−104.
(55) Pourcelly, G.; Sistat, P.; Chapotot, A.; Gavach, C.; Nikonenko, V. Self diffusion and conductivity in Nafion membranes in contact with NaCl + $CaCl_2$ solutions. *J. Membr. Sci.* **1996**, *110*, 69−78.
(56) Murata, T.; Tanioka, A. Ion transport across a polyelectrolyte-adsorbed cellulose triacetate membrane in the multicomponent ionic systems. *J. Colloid Interface Sci.* **1999**, *209*, 362−367.
(57) Chaudhury, S.; Agarwal, C.; Pandey, A. K.; Goswami, A. Self-diffusion of ions in Nafion-117 membrane having mixed ionic composition. *J. Phys. Chem. B* **2012**, *116*, 1605−1611.
(58) Kim, Y.; Walker, W. S.; Lawler, D. F. Competitive separation of di- vs. mono-valent cations in electrodialysis: Effects of the boundary layer properties. *Water Res.* **2012**, *46*, 2042−2056.
(59) Benavente, J.; Zhang, X.; Garcia Valls, R. Modification of polysulfone membranes with polyethylene glycol and lignosulfate: Electrical characterization by impedance spectroscopy measurements. *J. Colloid Interface Sci.* **2005**, *285*, 273−280.
(60) Park, J.-S.; Choi, J.-H.; Woo, J.-J.; Moon, S.-H. An electrical impedance spectroscopic (EIS) study on transport characteristics of ion-exchange membrane systems. *J. Colloid Interface Sci.* **2006**, *300*, 655−662.
(61) Dlugolecki, P.; Ogonowski, P.; Metz, S. J.; Saakes, M.; Nijmeijer, K.; Wessling, M. On the resistances of membrane, diffusion boundary layer and double layer in ion exchange membrane transport. *J. Membr. Sci.* **2010**, *349*, 369−379.
(62) Zhang, W.; Spichiger, U. E. An impedance study of Mg^{2+}-selective membranes. *Electrochim. Acta* **2000**, *45*, 2259−2266.
(63) Franceschetti, D. R.; Macdonald, J. R.; Buck, R. P. Interpretation of finite-length-Warburg-type impedances in supported and unsupported electrochemical cells with kinetically reversible electrodes. *J. Electrochem. Soc.* **1991**, *138*, 1368−1371.
(64) Jacobsen, T.; West, K. Diffusion impedance in planar, cylindrical and spherical symmetry. *Electrochim. Acta* **1995**, *40*, 255−262.
(65) Diard, J.-P.; Le Gorrec, B.; Montella, C. Linear diffusion impedance. General expression and applications. *J. Electroanal. Chem.* **1999**, *471*, 126−131.
(66) Freger, V. Diffusion impedance and equivalent circuit of a multilayer film. *Electrochem. Commun.* **2005**, *7*, 957−961.
(67) Bisquert, J.; García-Belmonte, G.; Fabregat-Santiago, F.; Bueno, P. R. Theoretical models for ac impedance of finite diffusion layers exhibiting low frequency dispersion. *J. Electroanal. Chem.* **1999**, *475*, 152−163.
(68) Sistat, P.; Pourcelly, G. Chronopotentiometric response of an ion-exchange membrane in the underlimiting current-range. Transport phenomena within the diffusion layers. *J. Membr. Sci.* **1997**, *123*, 121−131.
(69) Larchet, C.; Nouri, S.; Auclair, B.; Dammak, L.; Nikonenko, V. Application of chronopotentiometry to determine the thickness of diffusion layer adjacent to an ion-exchange membrane under natural convection. *Adv. Colloid Interface Sci.* **2008**, *139*, 45−61.
(70) Kozmai, A. E.; Nikonenko, V. V.; Pismenskaya, N. D.; Mareev, S. A.; Belova, E. I.; Sistat, P. Use of electrochemical impedance spectroscopy for determining the diffusion layer thickness at the surface of ion-exchanger membranes. *Pet. Chem.* **2012**, *52*, 614−624.
(71) Moya, A. A.; Sistat, P. Chronoamperometric response of ion-exchange membrane systems. *J. Membr. Sci.* **2013**, *444*, 412−419.
(72) Morf, W. E.; Pretsch, E.; De Rooij, N. F. Theoretical treatment and numerical simulation of potential and concentration profiles in extremely thin non-electroneutral membranes used for ion-selective electrodes. *J. Electroanal. Chem.* **2010**, *641*, 45−56.
(73) Sokalski, T.; Lewenstam, A. Application of Nernst-Planck and Poisson equations for interpretation of liquid-junction and membrane potentials in real-time and space domains. *Electrochem. Commun.* **2001**, *3*, 107−112.
(74) Post, J. W.; Hamelers, H. V. M.; Buuisman, C. J. N. Energy recovery from controlled mixing salt and fresh water with a reverse electrodialysis system. *Environ. Sci. Technol.* **2008**, *42*, 5785−5790.
(75) Dlugolecki, P.; Gambier, A.; Nijmeier, K.; Wessling, M. Practical potential of reverse electrodialysis as process for sustainable energy generation. *Environ. Sci. Technol.* **2009**, *43*, 6888−6894.
(76) Vermaas, D. A.; Saakes, M.; Nijmeijer, K. Doubled power density from salinity gradients at reduced intermembrane distance. *Environ. Sci. Technol.* **2011**, *45*, 7089−7095.
(77) Buck, R. P.; Mundt, C. Aperiodic equivalent circuit for charge permeable thin-layer cells of symmetric, asymmetric types. *J. Chem. Soc., Faraday Trans.* **1996**, *92*, 3947−3955.